Dual analysis of host and pathogen transcriptomes in ostreid herpesvirus 1-positive *Crassostrea gigas*

U. Rosani,[1] L. Varotto,[1] S. Domeneghetti,[1] G. Arcangeli,[2] A. Pallavicini[3†] and P. Venier[1*†]
[1]*Department of Biology, University of Padua, via U. Bassi 58/b, 35121 Padua, Italy.*
[2]*Istituto Zooprofilattico Sperimentale delle Venezie (IZSVe), via L. da Vinci 39, 45011 Adria, Italy.*
[3]*Department of Life Sciences, University of Trieste, via L. Giorgeri 5, 34127 Trieste, Italy.*

Summary

Ostreid herpesvirus type 1 (OsHV-1) has become a problematic infective agent for the Pacific oyster *Crassostrea gigas*. In particular, the OsHV-1 µVar subtype has been associated with severe mortality episodes in oyster spat and juvenile oysters in France and other regions of the world. Factors enhancing the infectivity of the virus and its interactions with susceptible and resistant bivalve hosts are still to be understood, and only few studies have explored the expression of oyster or viral genes during productive infections. In this work, we have performed a dual RNA sequencing analysis on an oyster sample with a high viral load. High sequence coverage allowed us to thoroughly explore the OsHV-1 transcriptome and identify the activated molecular pathways in *C. gigas*. The identification of several highly induced and defence-related oyster transcripts supports the crucial role played by the innate immune system against the virus and opportunistic microbes possibly contributing to subsequent spat mortality.

Introduction

Herpesviruses are a large group of viruses with a linear double-stranded DNA genome ranging in length from 110 to 230 kbp. Herpesviruses infect both vertebrate and invertebrate species and are divided into three main evolutionary groups: the first includes all characterized herpesviruses affecting mammalian, avian and reptilian hosts; the second group comprises fish and amphibian viruses; and the last group, the *Malacoherpesviridae*, infects only invertebrate hosts (Davison, 2010). In general, DNA viruses activate those host processes that are beneficial to their metabolic, anti-apoptotic and translational functions. During productive infections, viruses need also to overcome molecular pathways that enable infected cells to react and inhibit virus-sustained processes. The resulting intracellular signalling activates mechanisms that either reduce the infection intensity or induce definitive responses such as apoptotic cell death (Buchkovich *et al*., 2008). Ostreid herpesvirus type 1 (OsHV-1) was firstly associated with sporadic episodes of high mortality affecting larvae, spat and juveniles of the Pacific oyster (*Crassostrea gigas*) and some other marine mollusks (Arzul *et al*., 2001; Davison *et al*., 2005; Batista *et al*., 2007; Savin *et al*., 2010; Burge and Friedman, 2012; Renault *et al*., 2012). More recently, several mortality events associated to massive herpesvirus presence in *C. gigas* have been reported in Europe (Segarra *et al*., 2010; Renault *et al*., 2012; Roque *et al*., 2012; Lynch *et al*., 2013) and more distant regions worldwide (Burge *et al*., 2011; Grijalva-Chon *et al*., 2013; Hwang *et al*., 2013; Jenkins *et al*., 2013; Paul-Pont *et al*., 2014). Since 2008 (France), the oyster mortality outbreaks have been linked to a virulent OsHV-1 variant named µVar, commonly displaying a deletion of 12 nucleotides in the microsatellite locus H10 (Segarra *et al*., 2010; Renault *et al*., 2014). In addition to known polymorphisms mapping to open reading frame (ORF)4 and ORF43, other sequence changes have been reported in OsHV-1 specimens, including five large deletions and some single-nucleotide polymorphisms (SNPs) (Renault *et al*., 2012; Martenot *et al*., 2013).

The mortality of *C. gigas* seed represents a global problem that has spurred new research on the relationships between mollusk herpesviruses, especially OsHV-1 variants, and their hosts such as oysters, clams, scallops and abalones (Renault *et al*., 2001; Chang *et al*., 2005; Meyers *et al*., 2009; Ren *et al*., 2013). Using next-generation sequencing technologies, any organism can now be analysed like classical model species (Dheilly *et al*., 2014). In particular, the identification and characterization of immune-related gene transcripts is helping to elucidate the molecular pathways of innate defences in

Accepted 30 October, 2014.
*For correspondence. E-mail paola.venier@ unipd.it; Tel. +390498276284; Fax +390498276280. †Last authors.

many invertebrates including bivalves (Rauta *et al.*, 2014). In light of the recent release of the *C. gigas* oyster genome (Zhang *et al.*, 2012), there is the potential to define host responses to viruses using deep transcriptome sequencing. To date, the transcriptional responses of Pacific oyster to herpesvirus infection have been evaluated using a Digital Gene Expression approach (de Lorgeril *et al.*, 2011), SSH libraries (Renault *et al.*, 2011), DNA microarray (Jouaux *et al.*, 2013) and quantitative real-time polymerase chain reaction (qRT-PCR) (Green *et al.*, 2014; Normand *et al.*, 2014). Recently, the expression of 39 selected OsHV-1 ORFs and five host genes was measured by qRT-PCR in oyster spat up to 144 h after experimental infection with the virus (Segarra *et al.*, 2014a,b).

Our work aimed to identify and measure the expression of both host and OsHV-1 genes through dual RNA sequencing of an exceptional sample consisting of naturally infected oyster spat, later experiencing massive mortality. To our knowledge, this is the first simultaneous whole transcriptome analysis of *C. gigas* and OsHV-1. We analysed identity and absolute amounts of transcript sequences separately for the host and OsHV-1, thus investigating the simultaneous expression of viral genes and oyster defence genes during a naturally occurring host–pathogen interaction.

Results

OsHV-1 genome analysis

This study refers to one batch of *C. gigas* spat deployed in one lagoon site (Goro lagoon, North Adriatic Sea, Italy) found highly positive for OsHV-1-DNA on 21 May prior to the massive mortality occurred on 18 June 2012. The virus-positive oyster spat sampled in May is the only case encountered at the spring–summer transition during a 3-year survey performed on oysters and mussels co-cultured in baskets (Domeneghetti *et al.*, 2014). In detail, OsHV-1 DNA was detected in various amounts, up to 8.4×10^4 copies ng^{-1} DNA, in 30/30 oysters analysed by end-point and RT-PCR. In the same spat, notifiable pathogens were not detectable, but 1.5×10^7 and 7.6×10^6 cells of *Vibrio splendidus* and *Vibrio aestuarianus*, respectively, were recovered per gram of flesh. Based on high-throughput RNA sequencing, we now report the significant presence of viral transcripts in one RNA sample prepared from another 30 oysters of the same sampling (21 May 2012) in parallel.

Illumina transcriptome sequencing yielded more than 85 million reads with an average PHRED quality of 38. All of the 50 bp-paired reads were mapped against both the *C. gigas* and OsHV-1 genomes and subsequently used for gene expression counts. Nearly 71% of the total output reads, of which 81% mapped in pair, aligned on the *C. gigas* genome, whereas 3.08 million reads (3.6%) mapped to the OsHV-1 (AY509253) reference genome (Table 1). The latter reads covered almost all the viral genome, in amounts adequate for a deep expression analysis of the OsHV-1 genes (except for ORFs 34, 35 and 46). The average coverage resulted to be 718×, with a peak of 197 202 reads counted for ORF104; moreover, the GC content distribution of the oyster and viral reads did not overlap, in accordance with the different base composition of the two genomes (Fig. S1) (Davison *et al.*, 2005; Zhang *et al.*, 2013).

Table 1. Summary of the sequencing and read mapping.

a) Mapping	M reads	%	Mean CG (%)
Mapped on the Cg genome	60.4	70.7	45
Not mapped on the Cg genome	25.0	29.3	–
Mapped on the OsHV-1 genome	3.1	3.6	40
b) *De novo* assembling of viral reads	**M reads**	**%**	**Mean CG (%)**
Total reads	3.1	–	–
Assembled reads	3.0	99.95	–
Number of contigs	344	–	–
Average length	581	–	–
N50 (bp)	12 610	–	–

Once the reads of the OsHV-1 specimen detected in the Goro lagoon were mapped onto the reference genome, we analysed the spliced reads, paired distance and non-specific read matches in order to obtain precise information about deletions, insertions and single nucleotide changes (Fig. 1). Focusing on the previously identified polymorphic sites (Arzul *et al.*, 2001; Segarra *et al.*, 2010; Martenot *et al.*, 2013), we could confirm the presence of OsHV-1 μVar in the sequenced RNA sample.

We used all the viral reads to produce a *de novo* transcriptome assembly of the Goro lagoon μVar specimen, namely 344 contigs representing at least 124 viral ORFs over a length of 201 kbp, altogether constituting a reliable reference genome (Table 1b). By comparing the aligned viral reads with the reference genome (AY509253), we identified a total of 329 variations (94% not yet described; all showing > 99% representativeness) likely tracing the divergence between the reference OsHV-1 and our μVar specimen (Table S1). The most divergent ORFs were ORF3, ORF4, ORFs containing a RING domain (ORF9 and ORF124) and ORFs coding for membrane proteins. Among the less variable ORFs, we found sequences denoting other RING-domain containing proteins, primase, reductase, terminase and ORFs with transmembrane motifs. Moreover, in our OsHV-1 specimen, we identified polymorphic positions, mostly located inside the coding sequence (CDS) and leading to amino acid substitutions. The highest variation frequency was

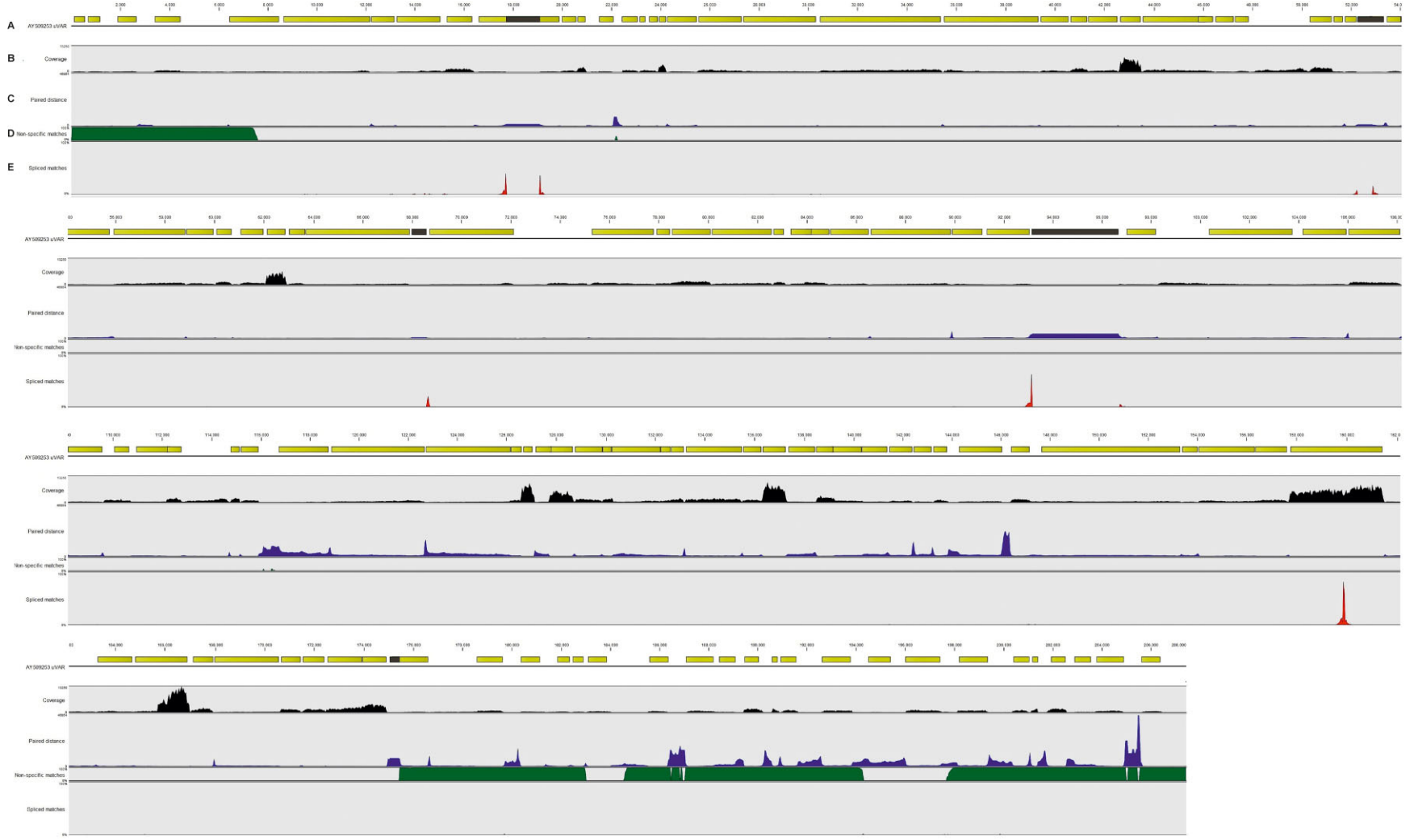

Fig. 1. Mapping the RNA-seq reads onto the OsHV-1 genome (AY509253). (A) Genome structure with ORFs in yellow and large deletions in light green (e.g. at 18 kbp). (B) Genome coverage. (C) Paired distance graph; regions with peak could be indicative of joined ORF transcription (e.g. at 115–145 kbp). (D) Non-specific matches highlight repeated genome regions (dark green) in which paired-reads analysis was impaired by the difficulty of assigning a unique read position; (E) spliced reads; a large number of spliced reads helps the recognition of small deletions (e.g. at 160 kbp).

Table 2. Viral ORFs with positive matches in *C. gigas* genome contigs.

ID	Description	E-value	Description	Position	Identity (%)	Hit length (bp)
OsHV1_gp048	Ribonucleotide reductase large subunit	9.42E-99	C36000, whole genome shotgun	2058–3917	50	1860
OsHV1_gp062	Class I membrane protein	1.68E-40	Scaffold266, whole genome shotgun	275 951–277 594	40.54	1650
OsHV1_gp080	BIR protein lacking RING finger	3.27E-29	Scaffold472, whole genome shotgun	28 461–28 973	52.78	543
OsHV1_gp111	Contains motifs V and VI characteristic of SF2 helicases	4.42E-26	C26364, whole genome shotgun	467–919	36.77	453
OsHV1_gp051	Class I membrane glycoprotein	3.55E-24	Scaffold42372, whole genome shotgun	33 652–34 602	34.82	1902
OsHV1_gp092	BIR protein lacking RING finger	3.35E-15	Scaffold808, whole genome shotgun	117 344–117 547	59.26	321
OsHV1_gp040	BIR protein containing RING finger	6.61E-15	Scaffold472, whole genome shotgun	28 533–28 973	55.26	552
OsHV1_gp061	SF2 helicase	4.44E-11	C26364, whole genome shotgun	668–1699	22.77	1032
OsHV1_gp098	BIR protein containing RING finger	4.14E-10	Scaffold808, whole genome shotgun	117 377–117 601	57.14	318

Sequence identity, function, genome localization and tblastn E-values are reported.

found in ORFs 16, 3, 122, 14 and 74, which refer to membrane proteins, secreted or unknown proteins. Finally, we identified a new deletion of nine nucleotides, located in ORF104 and occurring in 23% of aligned reads.

Based on the consensus sequences of membrane proteins, BIR domain-containing proteins, ORF36–37 region, IA1–IA2 and C2–C6 regions, we reconstructed the phylogenetic trees previously proposed by Martenot and colleagues (2013) and Renault and colleagues (2012). Despite all the sequence differences stated above, the new phylogenetic analyses, including the selected ORFs and sequence data from other authors, clearly located the North-Adriatic virus type in the subgroup of OsHV-1 microvariants (Fig. S2).

Protein domain analysis revealed the presence of 82 PFAM signatures in the viral ORFs. Expanding the analysis to the whole OsHV-1 genome translated in the six possible reading frames, we recognized a total of 286 protein domains. Because herpesviruses can occasionally integrate into the host genome (Arbuckle *et al*., 2010; Savin *et al*., 2010), we also checked all translated virus ORFs against the published *C. gigas* genome and identified some putatively integrated ostreid herpesvirus elements (Table 2).

Dual RNA sequencing analysis

The overall RNA sequencing (RNA-seq) output produced 85.4 M reads. Taking into account the total reads mapping onto the OsHV-1 genome (3.6%), the expression levels of the viral ORFs ranged from 480 to 197 202 reads per ORF (11 060 reads on average; Table S2). Such gene expression measurements are absolute values due to the absence of a proper control (the overall features of the lagoon site made it unique and allowed the OsHV-1 burst). In fact, additional RNA-seq data from similarly deployed oyster spat sampled in spring–summer 2011 and spring–summer 2013 (indicated as unpublished data in Table S3) did not contain any OsHV-1-related reads, notwithstanding the presence of trace amounts of viral DNA detectable by qRT-PCR in a minority of oysters per sample (Domeneghetti *et al*., 2014).

Among the most expressed viral ORFs, we found membrane proteins (ORFs 88, 80, 68, 77 and 41, in decreasing abundance), an inactive dUTPase (ORF27) and the viral DNA polymerase (ORF100) (Table 3). However, it should be recalled that many highly expressed viral proteins still have unknown functions, as previously reported in the expression analysis of other herpesviruses (Lisnic *et al*., 2013).

Table 3. Top 20 viral ORFs in decreasing order of expression value.

ID	ORF	Annotation	Total reads
OsHV1_gp097	104	Unknown	197 202
OsHV1_gp099	107	Unknown	94 270
OsHV1_gp083	90	Unknown	60 051
OsHV1_gp021	22	Unknown	43 168
OsHV1_gp026	27	Inactive dUTPase	42 514
OsHV1_gp043	45	Unknown	35 351
OsHV1_gp075	82	Unknown	33 080
OsHV1_gp081	88	Class I membrane protein	31 119
OsHV1_gp073	80	Membrane protein	30 192
OsHV1_gp105	113	Unknown	29 015
OsHV1_gp104	113	Unknown	24 843
OsHV1_gp093	100	DNA polymerase	21 109
OsHV1_gp027	28	Unknown	20 134
OsHV1_gp050	53	RING finger-like protein	20 124
OsHV1_gp062	68	Class I membrane protein	19 304
OsHV1_gp070	77	Class I membrane protein	18 572
OsHV1_gp031	33	Unknown	16 748
OsHV1_gp022	23	Unknown	16 714
OsHV1_gp039	41	Class I membrane protein	16 123
OsHV1_gp124	119	Unknown	15 316

Sequence identity, ORF number, putative annotation and total mapped reads are reported.

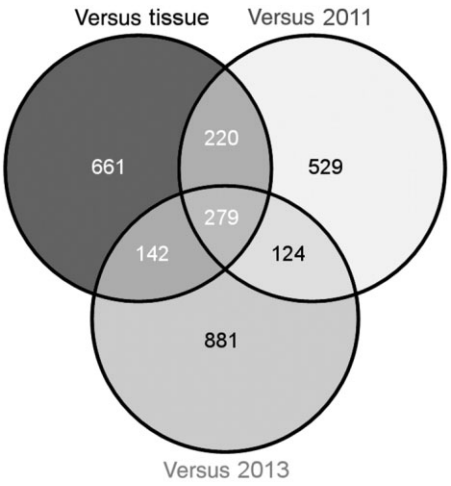

Fig. 2. Venn diagram of oyster DEGs obtained by comparing the RPKM values referred to the infected spat (CG1 gill sample) against samples from various tissues, 2011 gill samples and 2013 gill samples (fold change > 5).

After mapping and counting, the oyster RNA-seq reads were processed together with 13 additional RNA datasets from untreated *C. gigas*. According to the exploratory principal component analysis (PCA) (Fig. S3), the OSHV-1-positive oyster transcriptome set far apart from a cluster of seven tissue-specific RNA datasets from Zhang and colleagues (2012) and from two RNA dataset clusters generated from gills of spat deployed in the Goro lagoon in 2011 (6 months old, 3N) and 2013 (2–3 months old, 2N and very similar in size to the diploid oyster sample under study) (Table S3). Keeping in mind functional differences due to tissue, site of origin and sampling period, we decided to select the oyster transcripts ranked as differentially expressed genes (DEGs) by applying stringent parameters (fold change versus all groups > 5×) (Fig. 2): the 279 resulting oyster DEGs are displayed in Table S4, whereas Table 4 shows a selection of them proposed for discussion. These transcript sequences are genuine candidates whose role has to be understood and further validated as component of the antiviral oyster response.

Table 4. A selection of the most induced *C. gigas* genes.

ID	Symbol	Annotation	Average FC of induction	CG1 rank	'Control' rank
CGI_10024233	HAAF	Haemmaglutinin/amoebocyte aggregation factor	2866.9	10	10 818
CGI_10005220	C1q	Complement c1q tumor necrosis factor	5257.4	30	19 867
CGI_10003823	COMMD3	COMM-domain containing protein	69.8	119	7737
CGI_10019528	SOCS-2	Suppressor of cytokine signalling	25.8	154	3481
CGI_10016017	GEF	Guanine nucleotide exchange factor	81.2	217	12 610
CGI_10021170	IRF2	Interferon regulatory factor 2	10	231	2407
CGI_10018725	TFPI2	Tissue factor pathway inhib. 2	627	282	16 105
CGI_10021357	TRIM2	Tripartite motif-containing protein 2	219.7	321	22 778
CGI_10000144	UPF1	Regulator of nonsense transcripts 1-like	17.9	340	6242
CGI_10018396	RSAD	Viperin	14.8	433	6670
CGI_10012352	FSTL4	Follistatin	99.1	503	9154
CGI_10012998	ADAR	Double-stranded RNA specific adeno-deaminase	32.2	555	10 377
CGI_10012353	FSTL4	Follistatin	67.8	562	13 713
CGI_10003270	IRF8	Interferon regulatory factor 8	6.7	568	4625
CGI_10023765	Cd109	Cluster of differentiation 109	18.1	678	9266
CGI_10011954	INFi-44	Interferon induced protein 44	22.1	679	9065
CGI_10017857	ITIH3	Inter alpha trypsin inhibitor	587.9	760	17 647
CGI_10016615	EXD1	Exonuclease 3′–5′ domain containing protein 1	223.5	813	7658
CGI_10005392	BIRC3	Baculoviral IAP containing protein 3	22.6	962	17 281
CGI_10004837	IkB	Inhibitor of nuclear factor-kb	16.2	1006	15 065
CGI_10024671	BIRC2	Baculoviral IAP containing protein 2	6.2	1306	9562
CGI_10010566	imp1	Importin subunit α	41.6	1321	22 211
CGI_10002594	Hsp70	Heat shock protein 70	8.9	1826	14 541
CGI_10012722	MyD88	Myeloid differentiation primary response protein 88	16.7	2211	20 013
CGI_10011051	MMP3i	Matrix metalloproteinase 3 inhibitor	1570	2693	42 106
CGI_10013332	ANKRD50	Ankyrin repeat domain-containing prot. 50	7.4	2910	15 957
CGI_10028638	RND3	Rho related GTP binding protein	16.6	2949	21 726
CGI_10023661	–	Serine protease inhibitor dipetalogastin	144.8	3075	28 259
CGI_10028244	TRIM2	Tripartite motif-containing protein 2	8.6	3238	18 298
CGI_10001197	CSTA	Cystatin A1	188.6	3517	22 395
CGI_10005120	TRIM2	Tripartite motif-containing protein 2	29.8	3771	23 398
CGI_10011924	TRIM2	Tripartite motif-containing protein 2	7.6	3941	18 512
CGI_10007635	DEF	Big defensin	44.4	6119	30 577

We report sequence identity and symbol, functional annotation, average fold change of induction and rank order based on the whole transcriptome of either infected (CG1) or control (CG6) oyster spat. Underlined transcripts were also validated by qRT-PCR analysis.

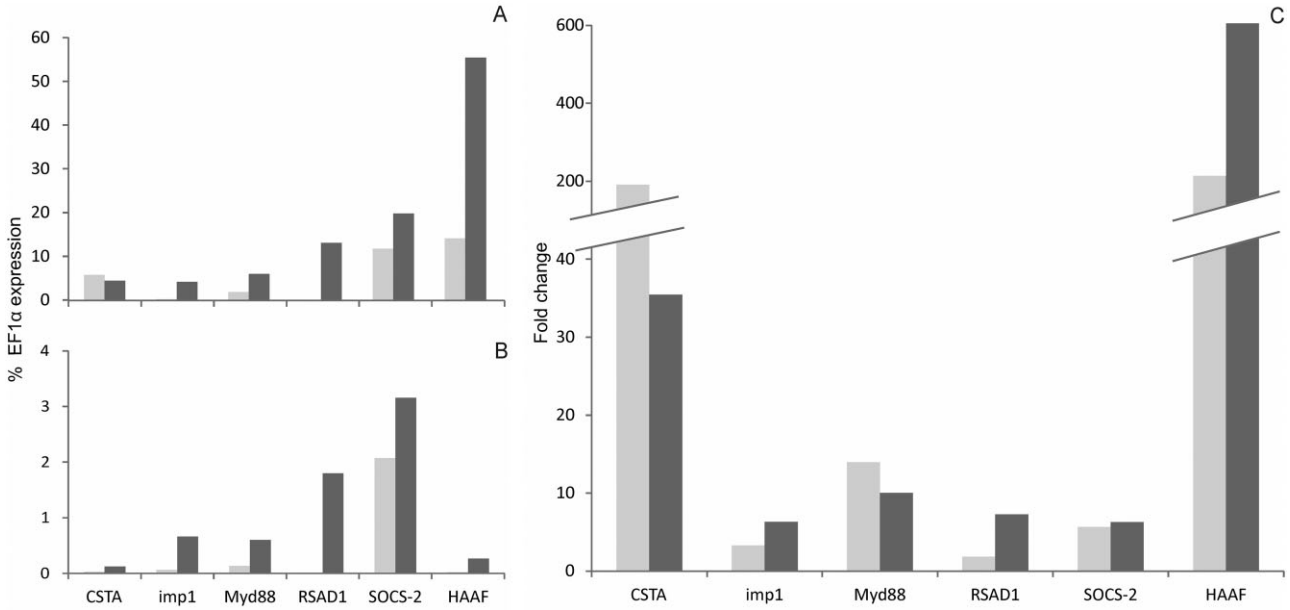

Fig. 3. Expression values of six oyster genes obtained by RNA-seq (dark grey) and RT-PCR (light grey). (A) Values detected in the spat infected in the Goro lagoon (CG1, gills) and (B) in control spat kept in laboratory tanks (CG6, gills); (C) fold change obtained by RNA-seq (dark grey) or RT-PCR (light grey) after normalization of all expression values to EF1α.

BLAST2GO annotation produced a blast hit in 58% of the oyster DEGs (161/279), with 92/279 (33%) coding genes annotated as 'hypothetical protein' with unknown function. Among the Gene Ontology categories, metabolic processes and response to stimuli emerged as the most perturbed ones, whereas other categories concerned virus-related pathways (Fig. S4). In detail, a number of DEGs reached an absolute expression level similar to that of housekeeping genes, namely haemagglutinin/amoebocyte aggregation factor, C1q/TNF, a COMM-domain containing protein and guanine nucleotide exchange factor (GEF), a guanine nucleotide exchange factor. The selection of genes proposed in Table 4 suggests an active host response, characterized by significant expression levels of transcripts typical although not exclusive of antiviral and antibacterial defences, like ADAR, IRF8, IRF2, IRF44, cystatins, a guanine nucleotide exchange factor and NFκB signalling pathway components.

The expression trends of six genes – selected for their different induction levels and absolute position in the oyster transcriptomes – were measured by qRT-PCR in both the infected sample (CG1) and a reference sample (CG6, diploid spat similar in size and maintained in tanks). As shown in Fig. 3A and B, target transcripts were confirmed at different abundance levels: from 55% of the EF1 alpha values (e.g. HAAF in the virus-positive spat of 2012, panel A) to 2–4% of the EF1α values (e.g. CSTA in reference spat of 2013, panel B). The expression trends measured by RNA-seq or qRT-PCR analysis were sufficiently coherent, except for RSAD1 and HAAF. The ratio of gene expression values of virus-infected oyster spat (2012) compared with the reference oyster spat (2013) emphasizes the over expression of HAAF, CSTA and Myd88 among the analysed gene transcripts (Fig. 3C).

Discussion

Dual sequencing of the host and pathogen transcriptomes offers an extraordinary opportunity to study molecular interactions occurring during a productive infection, with the advantage of avoiding the typical biases of other experimental approaches (Westermann *et al*., 2012; Hampton-Marcell *et al*., 2014).

The lophotrochozoan *C. gigas* is an important aquacultured bivalve, currently suffering from massive mortality events with significant economic losses worldwide. Such mortality outbreaks frequently occur in larvae and spat when seawater temperature rapidly exceeds 16–18°C and have been related to the presence of OsHV-1 in combination with other adverse factors, such as husbandry procedures, coexisting pathogenic *Vibrio spp*., changes in food quality and lower energy available for the oyster defences (Paul-Pont *et al*., 2013; Pernet *et al*., 2014; Wendling *et al*., 2014). In particular, the *C. gigas* mortalities recorded in France since 2008 and then in other regions of the world could be associated with particular viral specimens identified as OsHV-1 micro-variants (Segarra *et al*., 2010; Clegg *et al*., 2014;

Renault *et al*., 2014). Exploiting the feasibility of a dual RNA-seq experiment – which for the first time was performed in a marine bivalve during a productive viral infection – this work aimed to explore the transcriptional signatures of both OsHV-1 and the infected *C. gigas* spat. Because viral RNA is structurally identical to host transcripts, negative selection of viral transcripts during RNA extraction is prevented (Decroly *et al*., 2012).

The oyster spat collected on 21 May 2012 in the Goro lagoon (Italy) showed 100% prevalence of OsHV-1 DNA (30/30 positive oysters), and such evidence has been confirmed by the abundance of viral transcripts detected in the RNA extracted from another 30 oysters of the same sampling: around 3.6% of the sequenced reads positively mapped to the reference OsHV-1 genome (AY509253). This result suggests the exceptional presence of OsHV-1 in an active state as no other signs of infective OsHV-1 nor massive mortality have been recorded in the oysters deployed in the Goro lagoon at the spring–summer transition in the time of 3 years (Domeneghetti *et al*., 2014).

Trace amounts of OsHV-1 DNA were detected in a minor fraction of the oysters deployed in 2011 or 2013, a fact suggesting prior exposure to OsHV-1 (1–7 out of 30 analysed oysters per sampling harboured average values of 0.08–0.7 viral copies ng^{-1} DNA, irrespective of differences in size, ploidy and origin of the deployed oyster spat). Borderline levels of viral DNA were also detected in 3 of 12 spat survivors sampled on 18 June 2012 (Domeneghetti *et al*., 2014). These findings confirmed the dissemination of OsHV-1 also in the North Adriatic Sea and further suggest that only concomitant factors can trigger the lytic virus cycle from a more common dormant phase. As a matter of fact, massive oyster seed mortality associated to significant presence of OsHV-1 DNA was reported on 29 April 2013 in a local hatchery (Chioggia, Ve); nevertheless, product batches moved to other Italian coastal sites a short time before the mortality outbreak grew normally with the exception of a batch transferred to the Venice lagoon area and found dead just after a couple of days (P. Venier).

Many genomic regions have been analysed previously in various OsHV-1 specimens in order to identify variable sites and virus variants associated with oyster mortality (Segarra *et al*., 2010; Renault *et al*., 2012; 2014; Martenot *et al*., 2013). Updating the phylogenetic analysis previously performed on selected ORFs (Martenot *et al*., 2013) or other genome regions (Renault *et al*., 2012) for a total length of 25.7 kbp, we clearly placed the OsHV-1 specimen detected in the Goro lagoon among the microvariants, close to those observed in France and New Zealand (Keeling *et al*., 2014). The RNA-seq data allowed us to propose a complete OsHV-1 µVar reference genome, including at least 124 ORFs for a total length of 201 kbp.

The nucleotide differences occurring along the whole viral genome confirmed all the previously identified µVar features and indicated additional sequence variation sites. With regard to paired-read distance abnormalities and presence of spliced reads, we could identify five large deletions, in addition to the 12-nucleotide deletion previously reported, and a new nine-nucleotide deletion located on ORF104, i.e. a viral protein with unknown function. Moreover, the SNP analysis confirmed a high level of transcript polymorphism in membrane-related ORFs (ORFs 88, 41 and 77), whereas ORFs related to reductase and primase, expected to be evolutionary conserved, were almost invariant. Although protein glycosylation could have an important role also in OsHv-1 virulence (Vigerust and Shepherd, 2007) and a displacement of N-glycosylation sites has been observed previously (Martenot *et al*., 2013), we did not detect a similar situation in other highly variable membrane proteins. Overall, the molecular features of the OsHV-1 µVar detected in the Goro lagoon could be exploited to develop PCR-based protocols useful to discriminate this variant from other OsHV-1 subtypes.

According to the paired-read distances, some ORFs seem to be jointly transcribed as a long unique transcript and, moreover, the presence of many complete domains outside the CDS or in different reading frames supports the idea that OsHV-1 has a complex transcription machinery, not completely disclosed in other cases and never described in OsHV-1 (Stern-Ginossar *et al*., 2012; Krug, 2013; Lisnic *et al*., 2013; Moss and Steitz, 2013; Arias *et al*., 2014; Sijmons *et al*., 2014). We have also observed the integration of some viral elements in the oyster genome, described for the partially sequenced abalone herpesvirus (Savin *et al*., 2010). The identified integrated viral elements display similarity to proteins with conserved functions, also present in other bivalves (data not shown). As previously suggested by Savin and colleagues (2010), *in situ* genome hybridization could be the most interesting technique to confirm this finding.

The high and complete sequence coverage of the Goro lagoon OsHV-1 variant allowed us to perform an accurate and reliable ORF expression analysis despite the absence of a paired control or internal normalizer gene. The read counts indicated high levels of transcripts denoting many membrane proteins, DNA polymerase and identical expression levels of the two ribonucleotide reductase transcripts (large and small subunits) involved in DNA replication. Viral DNA polymerase is reported as an early response gene after infection (Beurden *et al*., 2013) including in OsHV-1 (Segarra *et al*., 2014a), and its high expression is likely to be essential to the infection progress. Because of the library preparation strategy, we

were not able to capture any microRNAs, which have been demonstrated to play important roles in other host–virus interactions (Murphy *et al*., 2008; Umbach and Cullen, 2010).

Regarding the oyster spat transcriptome, 13 heterogeneous RNA-seq samples from untreated *C. gigas* were included in the analysis as control samples in order to overcome the unavoidable lack of a paired control. We applied a stringent fold change filter to limit the intrinsic data variability and avoid biased classification of genes differentially expressed in the infected oyster spat. Overall, we identified 279 oyster DEGs, a number consistent with similar studies (Zhang *et al*., 2012; Jouaux *et al*., 2013).

During the infection, viruses fight against the host aiming to use the cell transcription machinery and reproduce themselves while overcoming multiple cell defence mechanisms. Looking at the most induced oyster genes, the activation of host defences was indicated by the abundance of transcripts for cytochrome P450, lectins, C1q and transcripts for big defensin, hsp70 and follistatin, the latter regarded as 'marker' of the innate immune responses (Miyamae *et al*., 2006; Murakami *et al*., 2012; Schmitt *et al*., 2012; Zhang *et al*., 2012). The activation of TLR/Nfkb signalling pathways in the infected oyster spat was confirmed by the high expression level of transcripts for TLR6, MyD88, IkB, COMM-domain containing protein and for several transcription factors (e.g. Friend leukaemia integration 1 transcription factor), also in line with other studies in which they observe similar genes overexpressed in a OsHV-1 susceptible oyster family after viral contact (Renault *et al*., 2011; Segarra *et al*., 2014b).

The active host defence was also suggested by the abundance of transcripts for a suppressor of cytokine signalling (SOCS2). In fact, suppression of cytokine pathways seems to be an important viral strategy to overcome the host defence system (Yokota *et al*., 2001; 2004). Abundance of transcripts for IRF2 and IRF8 interferon regulatory factors and the IRFi44 interferon-induced protein suggests the involvement of interferon-related pathways, one of the most effective antiviral defence mechanisms (Ozato *et al*., 2007; Randall and Goodbourn, 2008; Renault *et al*., 2011; Segarra *et al*., 2014b). The activation of interferon-like pathways in the oyster spat seems to be reinforced by the significant expression of the oyster homolog of viperin (radical s-adenosyl methionine domain containing protein 2): an interferon-inducible, iron-sulfur binding and antiviral protein that plays a major role during the antiviral response induced by many RNA and DNA viruses or poly I : C (Seo *et al*., 2011; Mattijssen and Pruijn, 2012; Green and Montagnani, 2013; Seo and Cresswell, 2013; Green *et al*., 2014). We also found as differentially expressed five interferon-inducible TRIM genes that are normally present in high copy number in various organisms (Ozato *et al*., 2007) and are involved in biological processes related to the innate immunity (Rajsbaum *et al*., 2008; Uchil *et al*., 2013).

In the infected oyster spat, several isoforms of the baculoviral IAP repeat containing protein BIRC, a multifunctional protein that regulates not only caspase expression and apoptosis but also the inflammatory signaling and immune responses, were also differentially expressed. Both viral and host IAPs were reported to be modulated following experimental infection of oysters with OsHV-1, with the oyster IAP transcripts being positively related to the viral DNA amounts in oyster families with contrasting susceptibility to the OsHV-1 infection (Segarra *et al*., 2014b).

Metalloproteinase activation and subsequent modulation of activity cytokine/chemokine and other proteins exemplify a way to overcome the viral proliferation (Zuo *et al*., 2014). Even if not present in DEGs, MMP3 was somewhat expressed only in the infected oyster spat. Conversely, other DEGs, like tissue factor pathway inhibitor 2 and inhibitor of MMPs (iMMPs), have a role in the control of metalloproteinase expression (Chand *et al*., 2005).

Among the most abundant oyster transcripts, we found a lectin able to aggregate amoebocytes and agglutinate erythrocytes (haemagglutinin/amoebocyte aggregation factor). The induction of a homologous gene was also observed in salmonid fish experimentally treated with bacteria (Gerwick *et al*., 2007; Renault *et al*., 2011).

Several oyster DEGs are related to apoptosis and suggest that apoptotic cell death is the most radical method to avoid viral proliferation; hence, the control of apoptotic signals is vital for the virus reproduction. Autophagy is a similar strategy to control and fight viruses, which in turn interfere with autophagy by targeting beclin1 to completely block autophagy or inhibit autophagosomal maturation. In the infected oyster spat, we observed the upregulation of GARP1 – an endogenous inhibitor of autophagy, able to bind beclin1 and act as antagonist of the pro-autophagy protein Nef (Deretic *et al*., 2013).

According to the model proposed by Jouaux and colleagues (2013) and data produced by Renault and colleagues (2011), the nuclear translocation of the virus can occur via the microtubular network, interacting with cytosolic actin filaments or by a importin-dependent pathway that involves the RAN complex formation (Giesen *et al*., 2000). Overexpression of genes denoting ADAR, exonuclease 3′-5′ domain containing protein, and UPF1, regulator of nonsense transcripts 1-like, suggested an intense RNA editing and degradation besides the improved stability of the viral DNA (Samuel, 2012; LeBlanc *et al*., 2013). In addition, the overexpressed

cystatin A1 may act as inhibitor of viral cysteine protease activities, thus inhibiting the delivery of the viral DNA into the nucleus (Peri *et al*., 2007; Kan *et al*., 2012).

The identification of 'marker' genes useful for tracking different organismal responses is of great interest in aquacultured bivalves. Regarding three genes recently proposed as putative markers of OsHV-1-resistant oysters (Normand *et al*., 2014), superoxide dismutase [Cu–Zn] was highly expressed but not modulated, NF-kappa-B inhibitor 2 was induced between 2 and 4 times, whereas dopamine D2 like receptor – similar to the dopamine receptor proposed as marker – was induced between 5 and 17 times in the infected oyster spat. Although single genes and signal pathways, such as NFκB, can be activated by stimuli other than viral and bacterial pathogens, the gene expression trends reported in this and other studies (Green and Montagnani, 2013; Segarra *et al*., 2014b) support further identification and validation of molecular markers to be used in the genetic selection of oyster stocks resistant to OsHV-1.

Selected oyster genes were tested by qRT-PCR to better understand our RNA-seq data. We chose transcripts presenting various expression levels, ranging from 10th to 3317th absolute position in the herpesvirus-positive sample and between the 3481th and 22 335th position in the analysed RNA samples considered as controls. The expression levels of the analysed genes were higher in the infected spat relative to a batch of control spat maintained on laboratory tanks, with fold change values obtained by RNA seq greater than those obtained by qPCR (the evident cystatin discrepancy may depend on not specific amplification of more than one isoform). The overall comparison makes us confident on the reliability of the whole transcriptome analysis.

Conclusion

In this work, we have performed a dual transcriptome analysis during a productive viral infection naturally occurred in *C. gigas* spat. Advanced RNA-seq allowed us to characterize the viral sample collected in the Goro lagoon as OsHV-1 micro-variant and supported the already published phylogenetic relationships between OsHV-1 specimens. Our findings reinforce the current knowledge on the virus–oyster interactions, i.e. the complex molecular events occurring between *C. gigas* spat and virulent ostreid herpesvirus variants. In this context, the innate immune responses of the host appear to play a major role. Of course we cannot exclude that *Vibrio* spp., able to persist in suitable niches of the marine environment and usually increasing in late spring, could have played a concurrent role in the observed transcriptional response of the oyster spat (Vezzulli *et al*., 2014). In the light of recent hypothesis, also viral elements of the oyster holobiont might influence the interactions between the bivalve host and its most known pathogens (Yvan *et al*., 2014). To the best of our knowledge, this is the first *in-vivo* application of a dual RNA-seq study in a marine bivalve related to a viral pathogen.

Experimental procedures

Sampled oysters, RNA extraction, library preparation and sequencing

Diploid *C. gigas* spat were deployed in a coastal lagoon of the Adriatic Sea in late spring (25 April 2012) for experimental purposes (Domeneghetti *et al*., 2014). After 26 days (21 May 2012), a sample of 30 oysters was collected (whole shell weight: 1.31 ± 0.40 g; major shell axes: 2.40 ± 0.30 cm, 1.55 ± 0.19; shell thickness: 0.68 ± 0.17 cm). The total flesh of individual oysters was immediately homogenized in 1 ml Trizol (Life Technologies, DE) using a T-10 Ultra-Turrax (IKA, Staufen, Germany) and frozen at −80°C until RNA extraction. Other subsamples of the same oyster batch were subjected to the molecular diagnosis of OsHV-1, *V. splendidus*, *V. aestuarianus* and to standard histology to evaluate the presence of notifiable pathogens (details in Domeneghetti *et al*., 2014).

Total RNA was extracted according to the manufacturer's instructions, quantified using the Qubit RNA BR Assay Kit (Life Technologies) and used to compose a unique RNA sample to be subjected to massive sequencing and qRT-PCR analysis. RNA quality was assessed with an Agilent Bioanalyzer 2100 (Agilent, Santa Clara, CA, USA). A cDNA library was prepared by retro-transcription of 1 μg of pooled RNA, using oligo(dT)12–18 (25 ng) and 200U of SuperScript II Reverse Transcriptase (Life Technologies). Dual transcriptome analysis was based on Illumina Hi-Seq2000 sequencing (2×50 bp reads, Epigenomics Core Facility; Cornell Medical College, NY, USA). Illumina reads are available in the ArrayExpress database (http://www.ebi.ac.uk/arrayexpress) under accession ID: E-MTAB-2552.

RNA-seq data analysis

The quality of sequencing readout was evaluated by the FastQC suite v0.11.1 (Biostars). Low-quality reads, with PHRED quality below 20 and more than two ambiguous nucleotides were eliminated. The reference oyster genome with the gene annotation proposed by Zhang and colleagues (2012) and OsHV-1 reference genome (AY509253) were downloaded from NCBI in complete gbk format (Davison *et al*., 2005; Zhang *et al*., 2012). In order to predict new transcripts and build a newly annotated genome for RNA-seq reference, the trimmed reads were firstly back mapped against the two reference genomes applying a large gap mapper algorithm to align the reads while allowing for large gaps. A deep analysis of the whole OsHV-1 genome was then performed to update the annotation of the viral genes. In detail, the distance of paired reads and the presence of spliced reads were evaluated against the OsHV-1 genome to detect large deletions or insertions; afterward, all the RNA-seq reads were back mapped to identify variable posi-

tions by a quality variant detection system based on the Neighborhood Quality Standard algorithm (Brockman *et al*., 2008). Subsequently, we counted the RNA-seq reads, mapping them onto either the oyster or OsHv-1 genomes and computed RPKM values (reads per kilobase per million mapped reads) for oyster or total mapped reads for OsHV-1. Quantile normalization was chosen to normalize the gene expression values, whereas the Baggerly test was used to associate a false discovery rate (FDR)-corrected *P*-value to each gene (Baggerly *et al*., 2003). We explored the transcriptome of the virus-positive (diploid) oysters without applying *a priori* hypothesis, comparing it by PCA with other *C. gigas* transcriptomes differing for tissue specificity of gene expression, life stage, ploidy and environment of origin (three RNA-seq groups, downloaded from the SRA archive or still unpublished, details in Fig. S5). As a result, oyster spat genes showing a fold change higher than five against all three RNA-seq groups were considered over expressed. In the absence of a proper control, such highly conservative cut-off was chosen to minimize the bias resulting from the heterogeneity of the SRA datasets selected for the comparison. Sequence processing and data analysis were performed with CLC GENOMIC WORKBENCH v.6 (Qiagen, Germany).

Expressed oyster genes and viral ORF analysis

All genes classified as DEGs were annotated with BLAST2GO (Conesa *et al*., 2005), with relevant information based on the BLASTn and Interpro databases. Reference OSHV-1 ORFs and ORF consensus sequences of the North Adriatic virus specimen detected in the present study were translated into amino acid sequences, scanned for signal peptide region with SIGNALP-3.0 (Petersen *et al*., 2011) and transmembrane domains with TMHMM v.2.0 (Krogh *et al*., 2001). Selected consensus sequences (membrane proteins: ORFs 16, 25, 32, 59, 65, 68, 72, 77, 80, 84, 88, 103 and 111; BIR proteins: ORFs 42, 106, 87 and 99; viral regions C, IAP and 36) were aligned together with publicly available reference sequences using CLUSTALW (Larkin *et al*., 2007). Phylogenetic analysis was performed using the maximum likelihood method with 1000 bootstraps, based on the Tamura Nei model distances using MEGA6 program (Tamura *et al*., 2013). Finally, the whole viral genome consensus was translated into the six possible reading frames and translations were scanned with HMMER3 (Eddy, 2011) against the PFAM database (Punta *et al*., 2012).

Real-time validation of gene expression trends

Owing to their expression levels, six oyster genes (Table S5) were selected for quantitative RT-PCR analysis, comparing the infected RNA (CG1) with a reference sample (CG6), diploid oyster spat of comparable size, maintained in control tanks and sampled on 11 Jun 2013). Preliminarily, we treated the samples with DNAse I (Qiagen, USA) to avoid the amplification of contaminant genomic DNA. One microlitre of purified and suitably diluted first-strand cDNAs was amplified in 10 μl of the following reaction solution: 1× SybrGreen PCR Master Mix (DyNAmoHS SybrGreen, Finnzymes, Italy), 1× Rox passive reference dye and 0.5 μM of each specific primer (listed in Table S5) using 96-well plates with a 7500 Real-Time PCR System (Applied Biosystems, Foster City, CA, USA). The applied thermal cycling conditions were: initial denaturation at 95°C for 15s; 40 cycles of denaturation at 95°C for 30s, annealing and elongation for 1m each at 60°C, and a final elongation at 72°C for 3m. All reactions were run in triplicate. In order to normalize RNA-seq expression data and qPCR Ct values, we selected the EF1α (NCBI ID: AB122066) as reference gene with the minimal variation in the sequenced samples, according to data produced in infected oyster spat (Segarra *et al*., 2014a,b).

Acknowledgements

The work has been developed in the frame of Bivalife (KBBE-2010-4-266157) granted by the EU FP7 Program. We are grateful to Sara Boscariol who kindly did the final linguistic revision.

References

Arbuckle, J.H., Medveczky, M.M., Luka, J., Hadley, S.H., Luegmayr, A., Ablashi, D., *et al*. (2010) The latent human herpesvirus-6A genome specifically integrates in telomeres of human chromosomes *in vivo and in vitro*. *Proc Natl Acad Sci USA* **107:** 5563–5568.

Arias, C., Weisburd, B., Stern-Ginossar, N., Mercier, A., Madrid, A.S., Bellare, P., *et al*. (2014) KSHV 2.0: a comprehensive annotation of the Kaposi's sarcoma-associated herpesvirus genome using next-generation sequencing reveals novel genomic and functional features. *PLoS Pathog* **10**(1)**:** e1003847.

Arzul, I., Renault, T., Lipart, C., and Davison, A.J. (2001) Evidence for interspecies transmission of oyster herpesvirus in marine bivalves. *J Gen Virol* **82:** 865–870.

Baggerly, K.A., Deng, L., Morris, J.S., and Aldaz, C.M. (2003) Differential expression in SAGE: accounting for normal between-library variation. *Bioinformatics* **19:** 1477–1483.

Batista, F.M., Arzul, I., Pepin, J.F., Ruano, F., Friedman, C.S., Boudry, P., and Renault, T. (2007) Detection of ostreid herpesvirus 1 DNA by PCR in bivalve molluscs: a critical review. *J Virol Methods* **139:** 1–11.

Beurden, S.J., Peeters, B.H., Rottier, P.J., Davison, A.Y., and Engelsma, M.Y. (2013) Genome-wide gene expression analysis of anguillid herpesvirus 1. *BMC Genomics* **14:** 83.

Brockman, W., Alvarez, P., Young, S., Garber, M., Giannoukos, G., Lee, W.L., *et al*. (2008) Quality scores and SNP detection in sequencing-by-synthesis systems. *Genome Res* **18:** 763–770.

Buchkovich, N.J., Yu, Y., Zampieri, C.A., and Alwine, J.C. (2008) The TORrid affairs of viruses: effects of mammalian DNA viruses on the PI3K–Akt–mTOR signalling pathway. *Nat Rev Microbiol* **6:** 266–275.

Burge, C.A., and Friedman, C.S. (2012) Quantifying ostreid herpesvirus (OsHV-1) genome copies and expression during transmission. *Microb Ecol* **63:** 596–604.

Burge, C.A., Strenge, R.E., and Friedman, C.S. (2011) Detection of the oyster herpesvirus in commercial bivalves in northern California, USA: conventional and quantitative PCR. *Dis Aquat Organ* **94:** 107–116.

Chand, H.S., Foster, D.C., and Walter, K. (2005) Structure, function and biology of tissue factor pathway inhibitor-2. *Thromb Haemost* **94:** 1122–1130.

Chang, P.H., Kuo, S.T., Lai, S.H., Yang, H.S., Ting, Y.Y., Hsu, C.L., and Chen, H.C. (2005) Herpes-like virus infection causing mortality of cultured abalone *Haliotis diversicolor* supertexta in Taiwan. *Dis Aquat Organ* **65:** 23–27.

Clegg, T.A., Morrissey, T., Geoghegan, F., Martin, S.W., Lyons, K., Ashe, S., and More, S.J. (2014) Risk factors associated with increased mortality of farmed Pacific oysters in Ireland during 2011. *Prev Vet Med* **113:** 257–267.

Conesa, A., Götz, S., García-Gómez, J.M., Terol, J., Talón, M., and Robles, M. (2005) Blast2GO: a universal tool for annotation, visualization and analysis in functional genomics research. *Bioinformatics* **21:** 3674–3676.

Davison, A.J. (2010) Herpesvirus systematics. *Vet Microbiol* **143:** 52–69.

Davison, A.J., Trus, B.L., Cheng, N., Steven, A.C., Watson, M.S., Cunningham, C., *et al*. (2005) A novel class of herpesvirus with bivalve hosts. *J Gen Virol* **86:** 41–53.

de Lorgeril, J., Zenagui, R., Rosa, R.D., Piquemal, D., and Bachère, E. (2011) Whole transcriptome profiling of successful immune response to vibrio infections in the oyster *Crassostrea gigas* by digital gene expression analysis. *PLoS ONE* **6:** e23142.

Decroly, E., Ferron, F., Lescar, J., and Canard, B. (2012) Conventional and unconventional mechanisms for capping viral mRNA. *Nat Rev Microbiol* **10:** 51–65.

Deretic, V., Saitoh, T., and Akira, S. (2013) Autophagy in infection, inflammation and immunity. *Nat Rev Immunol* **13:** 722–737. doi:10.1038/nri3532.

Dheilly, N.M., Adema, C., Raftos, D.A., Gourbal, B., Grunau, C., and Du Pasquier, L. (2014) No more non-model species: the promise of next generation sequencing for comparative immunology. *Dev Comp Immunol* **45:** 56–66.

Domeneghetti, S., Varotto, L., Civettini, M., Rosani, U., Stauder, M., Pretto, T., *et al*. (2014) Mortality occurrence and pathogen detection in *C. gigas* and *M. galloprovincialis* close-growing in shallow waters (Goro lagoon, Italy). *Fish Shellfish Immunol* **41**(1)**:** 37–44.

Eddy, S.R. (2011) Accelerated profile HMM searches. *PLoS Comput Biol* **7:** e1002195.

Gerwick, L., Corley-Smith, G., and Bayne, C.J. (2007) Gene transcript changes in individual rainbow trout livers following an inflammatory stimulus. *Fish Shellfish Immunol* **22:** 157–171.

Giesen, K., Radsak, K., and Bogner, E. (2000) The potential terminase subunit of human cytomegalovirus, pUL56, is translocated into the nucleus by its own nuclear localization signal and interacts with importin A. *J Gen Virol* **81:** 2231–2244.

Green, T.J., Montagnani, C. (2013) Poly I:C induces a protective antiviral immune response in the Pacific oyster (Crassostrea gigas) against subsequent challenge with Ostreid herpesvirus (OsHV-1 μvar). *Fish Shellfish Immunol* **35**(2): 382–388.

Green, T.J., Montagnani, C., Benkendorff, K., Robinson, N., and Speck, P. (2014) Ontogeny and water temperature influences the antiviral response of the Pacific oyster, *Crassostrea gigas*. *Fish Shellfish Immunol* **36:** 151–157.

Grijalva-Chon, J.M., Castro-Longoria, R., Ramos-Paredes, J., Enríquez-Espinoza, T.L., and Mendoza-Cano, F. (2013) Detection of a new OsHV-1 DNA strain in the healthy Pacific oyster, *Crassostrea gigas* Thunberg, from the Gulf of California. *J Fish Dis* **36:** 965–968.

Hampton-Marcell, J.T., Moormann, S.M., Owens, S.M., and Gilbert, J.A. (2014) Preparation and metatranscriptomic analyses of host-microbe systems. *Methods Enzymol* **531:** 169–185.

Hwang, J.Y., Park, J.J., Yu, H.J., Hur, Y.B., Arzul, I., Couraleau, Y., and Park, M.A. (2013) Ostreid herpesvirus 1 infection in farmed Pacific oyster larvae *Crassostrea gigas* (Thunberg) in Korea. *J Fish Dis* **36:** 969–972.

Jenkins, C., Hick, P., Gabor, M., Spiers, Z., Fell, S.A., Gu, X., *et al*. (2013) Identification and characterisation of an ostreid herpesvirus-1 microvariant (OsHV-1 μ-var) in *Crassostrea gigas* (Pacific oysters) in Australia. *Dis Aquat Organ* **105:** 109–126.

Jouaux, A., Lafont, M., Blin, J.L., Houssin, M., Mathieu, M., and Lelong, C. (2013) Physiological change under OsHV-1 contamination in Pacific oyster *Crassostrea gigas* through massive mortality events on fields. *BMC Genomics* **14:** 590.

Kan, Y., Okabayashi, T., Yokota, S., Yamamoto, S., Fujii, N., and Yamashita, T. (2012) Imiquimod suppresses propagation of herpes simplex virus 1 by upregulation of cystatin A via the adenosine receptor A1 pathway. *J Virol* **86:** 10338–10346.

Keeling, S.E., Brosnahan, C.L., Williams, R., Gias, E., Hannah, M., Bueno, R., *et al*. (2014) New Zealand juvenile oyster mortality associated with ostreid herpesvirus 1 – an opportunistic longitudinal study. *Dis Aquat Organ* **109:** 231–239.

Krogh, A., Larsson, B., von Heijne, G., and Sonnhammer, E.L. (2001) Predicting transmembrane protein topology with a hidden markov model: application to complete genomes. *J Biochem Mol Biol* **305:** 567–580.

Krug, L.T. (2013) Complexities of gammaherpesvirus transcription revealed by microarrays and RNAseq. *Curr Opin Virol* **3:** 276–284.

Larkin, M.A., Blackshields, G., Brown, N.P., Chenna, R., McGettigan, P.A., McWilliam, H., *et al*. (2007) Clustal W and clustal X version 2.0. *Bioinformatics* **23:** 2947–2948.

LeBlanc, J., Weil, J., and Beemon, K. (2013) Posttranscriptional regulation of retroviral gene expression: primary RNA transcripts play three roles as pre-mRNA, mRNA, and genomic RNA. *Wiley Interdiscip Rev RNA* **4**(5)**:** 567–580.

Lisnic, J.V., Cac, M.B., Lisnic, B., Trsan, T., Mefferd, A., Mukhopadhyay, C.D., *et al*. (2013) Dual analysis of the murine cytomegalovirus and host cell transcriptomes reveal new aspects of the virus-host cell interface. *PLoS Pathog* **9:** e1003611.

Lynch, S.A., Dillane, E., Carlsson, J., and Culloty, S.C. (2013) Development and assessment of a sensitive and cost-effective polymerase chain reaction to detect ostreid herpesvirus 1 and variants. *J Shellfish Res* **32:** 657–664.

Martenot, C., Travaillé, E., Lethuillier, O., Lelong, C., and Houssin, M. (2013) Genome exploration of six variants of

the ostreid herpesvirus 1 and characterization of large deletion in OsHV-1μVar specimens. *Virus Res* **178:** 462–470.

Mattijssen, S., and Pruijn, G.J. (2012) Viperin, a key player in the antiviral response. *Microbes Infect* **14:** 419–426.

Meyers, T.R., Burton, T., Evans, W., and Starkey, N. (2009) Detection of viruses and virus-like particles in four species of wild and farmed bivalve molluscs in Alaska, USA, from 1987 to 2009. *Dis Aquat Organ* **88:** 1–12.

Miyamae, T., Marinov, A.D., Sowders, D., Wilson, D.C., Devlin, J., Boudreau, R., *et al*. (2006) Follistatin-like protein-1 is a novel proinflammatory molecule. *J Immunol* **177:** 4758–4762.

Moss, W.N., and Steitz, J.A. (2013) Genome-wide analyses of Epstein-Barr virus reveal conserved RNA structures and a novel stable intronic sequence RNA. *BMC Genomics* **14:** 543.

Murakami, K., Tanaka, M., Usui, T., Kawabata, D., Shiomi, A., Iguchi-Hashimoto, M., *et al*. (2012) Follistatin-related protein/follistatin-like 1 evokes an innate immune response via CD14 and toll-like receptor 4. *FEBS Lett* **586:** 319–324.

Murphy, E., Vaníček, J., Robins, H., Shenk, T., and Levine, A.J. (2008) Suppression of immediate-early viral gene expression by herpesvirus-coded microRNAs: implications for latency. *Proc Natl Acad Sci USA* **105:** 5453–5458.

Normand, J., Li, R., Quillien, V., Nicolas, J.L., Boudry, P., Pernet, F., and Huvet, A. (2014) Contrasted survival under field or controlled conditions displays associations between mRNA levels of candidate genes and response to OsHV-1 infection in the Pacific oyster *Crassostrea gigas*. *Mar Genomics* **15:** 95–102.

Ozato, K., Tailor, P., and Kubota, T. (2007) The interferon regulatory factor family in host defense: mechanism of action. *J Biol Chem* **282:** 20065–20069.

Paul-Pont, I., Dhand, N.K., and Whittington, R.J. (2013) Spatial distribution of mortality in Pacific oysters *Crassostrea gigas*: reflection on mechanisms of OsHV-1 transmission. *Dis Aquat Organ* **105:** 127–138.

Paul-Pont, I., Evans, O., Dhand, N.K., Rubio, A., Coad, P., and Whittington, R.J. (2014) Descriptive epidemiology of mass mortality due to ostreid herpesvirus-1 (OsHV-1) in commercially farmed Pacific oysters (*Crassostrea gigas*) in the Hawkesbury River estuary, Australia. *Aquaculture* **422–423:** 146–159.

Peri, P., Hukkanen, V., Nuutila, K., Saukko, P., Abrahamson, M., and Vuorinen, T. (2007) The cysteine protease inhibitors cystatins inhibit herpes simplex virus type 1-induced apoptosis and virus yield in HEp-2 cells. *J Gen Virol* **88** (Part 8): 2101–2105.

Pernet, F., Lagarde, F., Jeannée, N., Daigle, G., Barret, J., Le Gall, P., *et al*. (2014) Spatial and temporal dynamics of mass mortalities in oysters is influenced by energetic reserves and food quality. *PLoS ONE* **9:** e88469.

Petersen, T.N., Brunak, S., von Heijne, G., and Nielsen, H. (2011) SignalP 4.0: discriminating signal peptides from transmembrane regions. *Nat Methods* **8:** 785–786.

Punta, M., Coggill, P.C., Eberhardt, R.Y., Mistry, J., Tate, J., Boursnell, C., *et al*. (2012) The Pfam protein families database. *Nucleic Acids Res* **40** (D1): D290–D301.

Rajsbaum, R., Stoye, J.P., and O'Garra, A. (2008) Type I interferon-dependent and -independent expression of tripartite motif proteins in immune cells. *Eur J Immunol* **38:** 619–630.

Randall, R.E., and Goodbourn, S. (2008) Interferons and viruses: an interplay between induction, signalling, antiviral responses and virus countermeasures. *J Gen Virol* **89:** 1–47.

Rauta, P.R., Samanta, M., Dash, H.R., Nayak, B., and Das, S. (2014) Toll-like receptors (TLRs) in aquatic animals: signaling pathways, expressions and immune responses. *Immunol Lett* **158:** 14–24.

Ren, W., Chen, H., Renault, T., Cai, Y., Bai, C., Wang, C., and Huang, J. (2013) Complete genome sequence of acute viral necrosis virus associated with massive mortality outbreaks in the Chinese scallop, *Chlamys farreri*. *Virol J* **10:** 110.

Renault, T., Lipart, C., and Arzul, I. (2001) A herpes-like virus infecting *Crassostrea gigas* and *Ruditapes philippinarum* larvae in France. *J Fish Dis* **24:** 369–376.

Renault, T., Faury, N., Barbosa-Solomieu, V., and Moreau, K. (2011) Suppression substractive hybridisation (SSH) and real time PCR reveal differential gene expression in the Pacific cupped oyster, *Crassostrea gigas*, challenged with ostreid herpesvirus 1. *Dev Comp Immunol* **35:** 725–735.

Renault, T., Moreau, P., Faury, N., Pepin, J.F., Segarra, A., and Webb, S. (2012) Analysis of clinical ostreid herpesvirus 1 (Malacoherpesviridae) specimens by sequencing amplified fragments from three virus genome areas. *J Virol* **86:** 5942–5947.

Renault, T., Tchaleu, G., Faury, N., Moreau, P., Segarra, A., Barbosa-Solomieu, V., and Lapegue, S. (2014) Genotyping of a microsatellite locus to differentiate clinical ostreid herpesvirus 1 specimens. *Vet Res* **45:** 3.

Roque, A., Carrasco, N., Andree, K.B., Lacuesta, B., Elandaloussi, L., Gairin, I., *et al*. (2012) First report of OsHV-1 microvar in Pacific oyster (*Crassostrea gigas*) cultured in Spain. *Aquaculture* **324–325:** 303–306.

Samuel, C.E. (2012) ADARs, viruses and innate immunity. *Curr Top Microbiol Immunol* **353:** 163–195.

Savin, K.W., Cocks, B.G., Wong, F., Sawbridge, T., Cogan, N., Savage, D., and Warner, S. (2010) A neurotropic herpesvirus infecting the gastropod, abalone, shares ancestry with oyster herpesvirus and a herpesvirus associated with the amphioxus genome. *Virol J* **7:** 308.

Schmitt, P., Rosa, R.D., Duperthuy, M., de Lorgeril, J., Bachere, E., and Destoumieux-Garzon, D. (2012) The antimicrobial defense of the Pacific oyster, Crassostrea gigas. How diversity may compensate for scarcity in the regulation of resident/pathogenic microflora. *Front Microbiol* **3:** 160.

Segarra, A., Pépin, J.F., Arzul, I., Morga, B., Faury, N., and Renault, T. (2010) Detection and description of a particular ostreid herpesvirus 1 genotype associated with massive mortality outbreaks of Pacific oysters, *Crassostrea gigas*, in France in 2008. *Virus Res* **153:** 92–99.

Segarra, A., Faury, N., Pépin, J.F., and Renault, T. (2014a) Transcriptomic study of 39 ostreid herpesvirus 1 genes during an experimental infection. *J Invertebr Pathol* **119:** 5–11.

Segarra, A., Mauduit, F., Faury, N., Trancart, S., Dégremont, L., Tourbiez, D., *et al*. (2014b) Dual transcriptomics of virus-host interactions: comparing two Pacific oyster families presenting contrasted susceptibility to ostreid herpesvirus 1. *BMC Genomics* **15:** 580.

Seo, J., and Cresswell, P. (2013) Viperin regulates cellular lipid metabolism during human cytomegalovirus infection. *PLoS Pathog* **9:** e1003497.

Seo, J., Yaneva, R., Hinson, E.R., and Cresswell, P. (2011) Human cytomegalovirus directly induces the antiviral protein viperin to enhance infectivity. *Science* **332:** 1093–1097.

Sijmons, S., Van Ranst, M., and Maes, P. (2014) Genomic and functional characteristics of human cytomegalovirus revealed by next-generation sequencing. *Viruses* **6:** 1049–1072.

Stern-Ginossar, N., Weisburd, B., Michalski, A., Le, V.T., Hein, M.Y., Huang, S., *et al*. (2012) Decoding human cytomegalovirus. *Science* **338**(6110)**:** 1088–1093.

Tamura, K., Stecher, G., Peterson, D., Filipski, A., and Kumar, S. (2013) MEGA6: Molecular Evolutionary Genetics Analysis version 6.0. *Mol Biol Evol* **30:** 2725–2729.

Uchil, P.D., Hinz, A., Siegel, S., Coenen-Stass, A., Pertel, T., Luban, J., and Mothes, W. (2013) TRIM protein-mediated regulation of inflammatory and innate immune signaling and its association with antiretroviral activity. *J Virol* **87:** 257–272.

Umbach, J.L., and Cullen, B.R. (2010) In-depth analysis of Kaposi's sarcoma-associated herpesvirus microRNA expression provides insights into the mammalian microRNA-processing machinery. *J Virol* **84:** 695–703.

Vezzulli, L., Pezzati, E., Stauder, M., Stagnaro, L., Venier, P., and Pruzzo, C. (2014) Aquatic ecology of the oyster pathogens *Vibrio splendidus* and *Vibrio aestuarianus*. *Environ Microbiol* Environ Microbiol [Epub ahead of print] doi: 10.1111/1462-2920.12484.

Vigerust, D.J., and Shepherd, V.L. (2007) Virus glycosylation: role in virulence and immune interactions. *Trends Microbiol* **15:** 211–218.

Wendling, C.C., Batista, F.M., and Wegner, K.M. (2014) Persistence, seasonal dynamics and pathogenic potential of *Vibrio* communities from Pacific oyster hemolymph. *PLoS ONE* **9:** e94256.

Westermann, A.J., Gorski, S.A., and Vogel, J. (2012) Dual RNA-seq of pathogen and host. *Nat Rev Microbiol* **10:** 618–630.

Yokota, S., Yokosawa, N., Okabayashi, T., Suzutani, T., Miura, S., Jimbow, K., and Fujii, N. (2001) Herpes simplex virus type 1 suppresses the interferon signaling pathway by inhibiting phosphorylation of STATs and janus kinases during an early infection stage. *Virology* **286:** 119–124.

Yokota, S., Yokosawa, N., Okabayashi, T., Suzutani, T., Miura, S., Jimbow, K., and Fujii, N. (2004) Induction of suppressor of cytokine signaling-3 by herpes simplex virus type 1 contributes to inhibition of the interferon signaling pathway. *J Virol* **78:** 6282–6286.

Yvan, B., Bouvier, T., Nguyen, H.K., and Thu, P.T. (2014) The versatile nature of coral-associated viruses. *Environ Microbiol* [Epub ahead of print] doi: 10.1111/1462-2920.12579.

Zhang, G., Fang, X., Guo, X., Li, L., Luo, R., Xu, F., *et al*. (2012) The oyster genome reveals stress adaptation and complexity of shell formation. *Nature* **490:** 49–54.

Zhang, Y., He, X., Yu, F., Xiang, Z., Li, J., Thorpe, K.L., and Yu, Z. (2013) Characteristic and functional analysis of toll-like receptors (TLRs) in the lophotrocozoan, *Crassostrea gigas*, reveals ancient origin of TLR-mediated innate immunity. *PLoS ONE* **8:** e76464.

Zuo, X., Pan, W., Feng, T., Shi, X., and Dai, J. (2014) Matrix metalloproteinase 3 promotes cellular anti-dengue virus response via interaction with transcription factor NF? B in cell nucleus. *PLoS ONE* **9:** e84748.

Supporting information

Additional Supporting Information may be found in the online version of this article

Fig. S1. Distribution of the CG content in the oyster reads (blue, 70% of Illumina reads) and viral reads (red, 3.6% of the total output reads).

Fig. S2. OsHV-1 phylogenetic trees based on (A) membrane proteins, (B) BIR domain containing proteins, (C) ORF36-37 region, (D) IA1-IA2 region and (E) C2-C6 region. Sample acronyms include date and location of the viral isolates ('Italy 2012' refers to this study).

Fig. S3. Principal component analysis of 14 oyster RNA-seq samples, namely the present dataset (in red, whole flesh), Zhang and colleagues (2012) dataset (in green, seven tissues) and unpublished datasets from 2011 (in blue, gills) and 2013 (in yellow, gills).

Fig. S4. Synopsis of the cell processes emerging from the analysis of the *C. gigas* DEGs.

Table S1. Sequence changes detected in the viral reads mapped against the OsHV-1 reference genome. The already described variations are highlighted in green.

Table S2. Expression values of all the ORFs (124) of the Goro lagoon OsHV-1 specimen. ORF, annotation, total mapped reads, RPKM values and ORF length are reported.

Table S3. RNA-seq samples used in the comparative gene expression analysis.

Table S4. RPKM values of all *C. gigas* genes showing differential expression in relation to the SM8 datasets (279 DEGs). Gene ID, fold changes obtained comparing the analysed sample with the 3 RNA-seq groups (tissues, 2011 and 2013), respective expression values and annotations.

Table S5. List of primer pairs used for RT-PCR analysis.